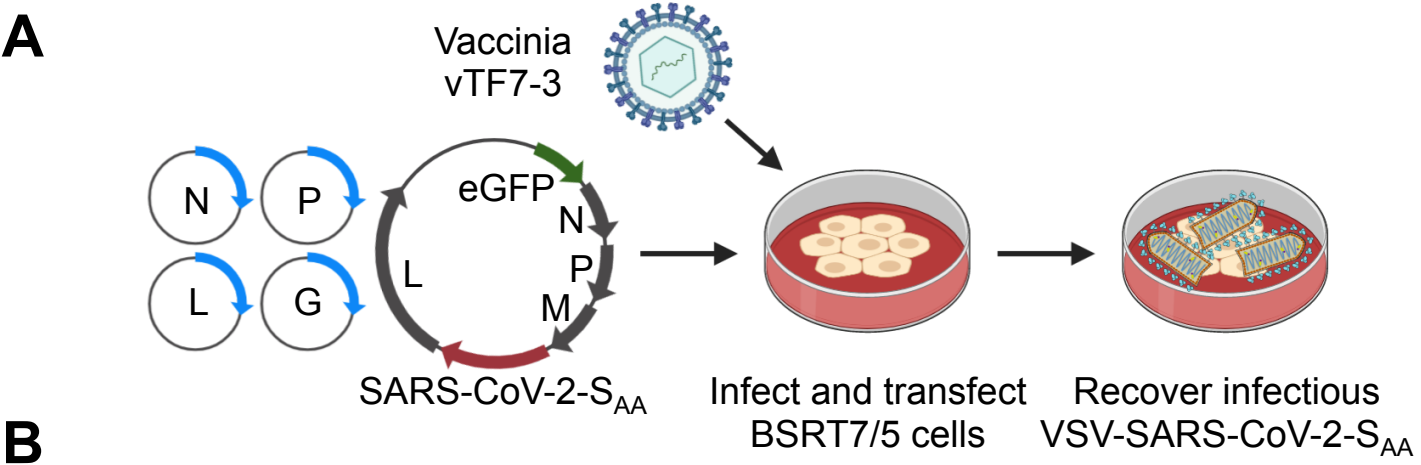**Supplemental Information**
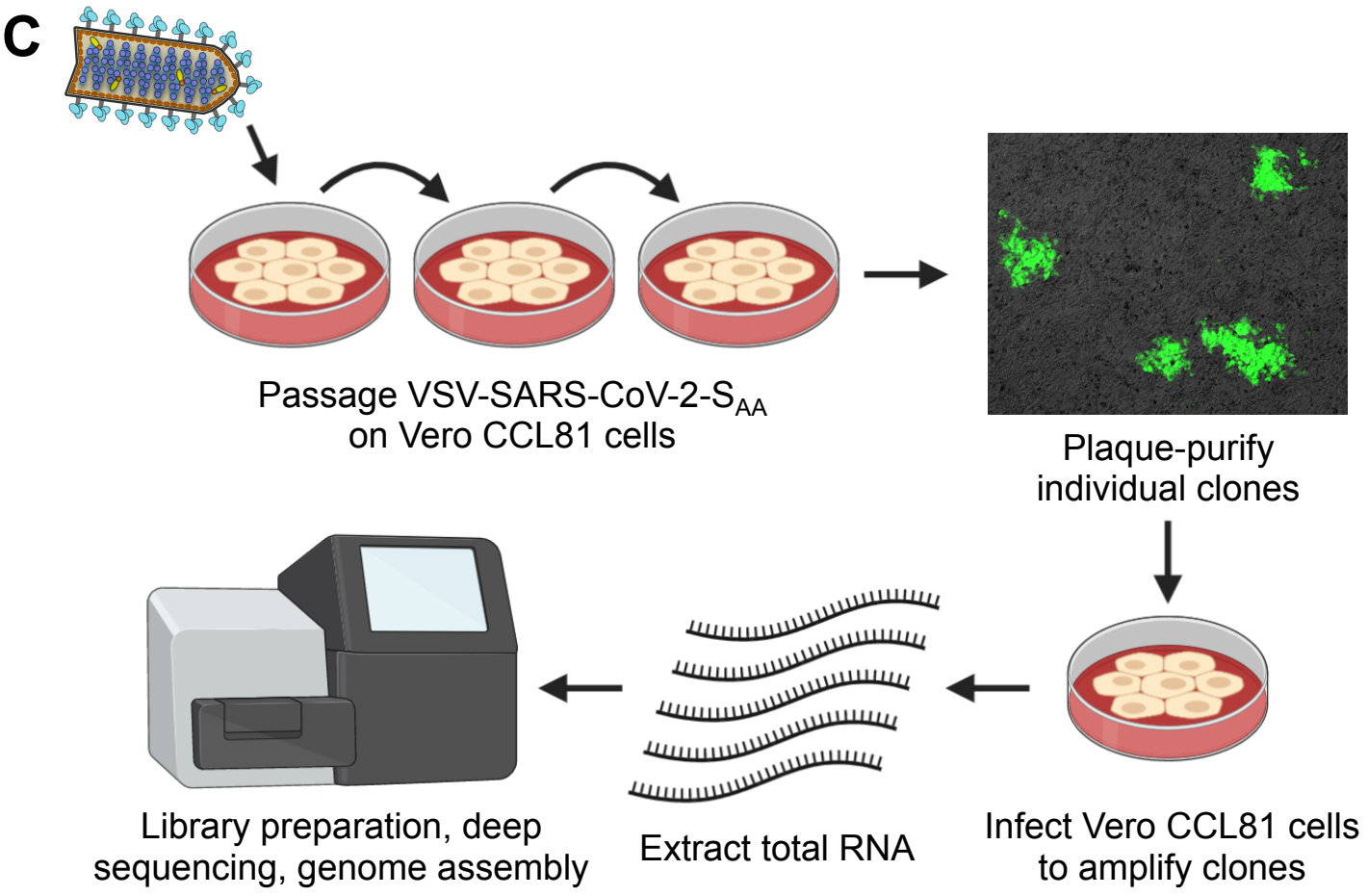

Neutralizing Antibody and Soluble ACE2 Inhibition

of a Replication-Competent VSV-SARS-CoV-2

and a Clinical Isolate of SARS-CoV-2

James Brett Case, Paul W. Rothlauf, Rita E. Chen, Zhuoming Liu, Haiyan Zhao, Arthur S. Kim, Louis-Marie Bloyet, Qiru Zeng, Stephen Tahan, Lindsay Droit, Ma. Xenia G. Ilagan, Michael A. Tartell, Gaya Amarasinghe, Jeffrey P. Henderson, Shane Miersch, Mart Ustav, Sachdev Sidhu, Herbert W. Virgin, David Wang, Siyuan Ding, Davide Corti, Elitza S. Theel, Daved H. Fremont, Michael S. Diamond, and Sean P.J. Whelan

A Vaccinia vTF7-3

N P L G — eGFP, N, P, M, L — SARS-CoV-2-S$_{AA}$

Infect and transfect BSRT7/5 cells → Recover infectious VSV-SARS-CoV-2-S$_{AA}$

B

Tail Mutant	Amino acid sequence (membrane proximal region, transmembrane domain, cytoplasmic tail)	Rescue	Spread
S$_{AA}$	LNESLIDLQELGKYEQYIKWPWYIWLGFIAGLIAIVMVTIMLCCMTSCCSCLKGCCSCGSCCKFDEDDSEPVLKGVALAYT	+	+
MERS S$_{AA}$	LNESLIDLQELGKYEQYIKWPWYIWLGFIAGLIAIVMVTIMLKLKCNRCCDRYEEYDLEPHAVAVH	+	-
VSV G #1	LNESLIDLQELGKYEQYIKWPWYIWLGFIAGLIAIVMVTIMLCCMTSCCSCLRVGIYLCIKLKHTKKRQIYTDIEMNRLGK	+	-
VSV G #2	LNESLIDLQELGKYEQYIKWPWYIWLGFIAGLIAIVMVTIMLRVGIYLCIKLKHTKKRQIYTDIEMNRLGK	+	-
VSV G TM/tail	LNESLIDLQELGKYEQYIKWSSIASFCFIIGLIIGLFLVLRVGIYLCIKLKHTKKRQIYTDIEMNRLGK	+	-
VSV G Ecto/TM/tail	LNEGWFSSWKSSIASFCFIIGLIIGLFLVLRVGIYLCIKLKHTKKRQIYTDIEMNRLGK	+	-

C

Passage VSV-SARS-CoV-2-S$_{AA}$ on Vero CCL81 cells → Plaque-purify individual clones → Infect Vero CCL81 cells to amplify clones → Extract total RNA → Library preparation, deep sequencing, genome assembly

Figure S1. Rescue of a chimeric VSV expressing the SARS-CoV-2 S protein and forward genetic selection of a gain-of-function mutant, Related to Figure 1. (**A**) BSRT7/5 cells were infected with vaccinia virus vTF7-3, transfected with plasmids allowing T7-driven expression of VSV N, P, L, and G, and an infectious molecular cDNA of VSV-SARS-CoV-2-S$_{AA}$ to produce replication-competent VSV-SARS-CoV-2-S$_{AA}$. (**B**) Alignment of the membrane proximal region, transmembrane domain, and cytoplasmic tail of various recombinants that were generated. Successful rescue and indication of spread are noted. (**C**) VSV-SARS-CoV-2-S$_{AA}$ was passaged iteratively on Vero CCL81 cells. Several clones were plaque-purified and amplified on Vero CCL81 cells. RNA from infected cells was extracted and deep sequenced to identify mutants.
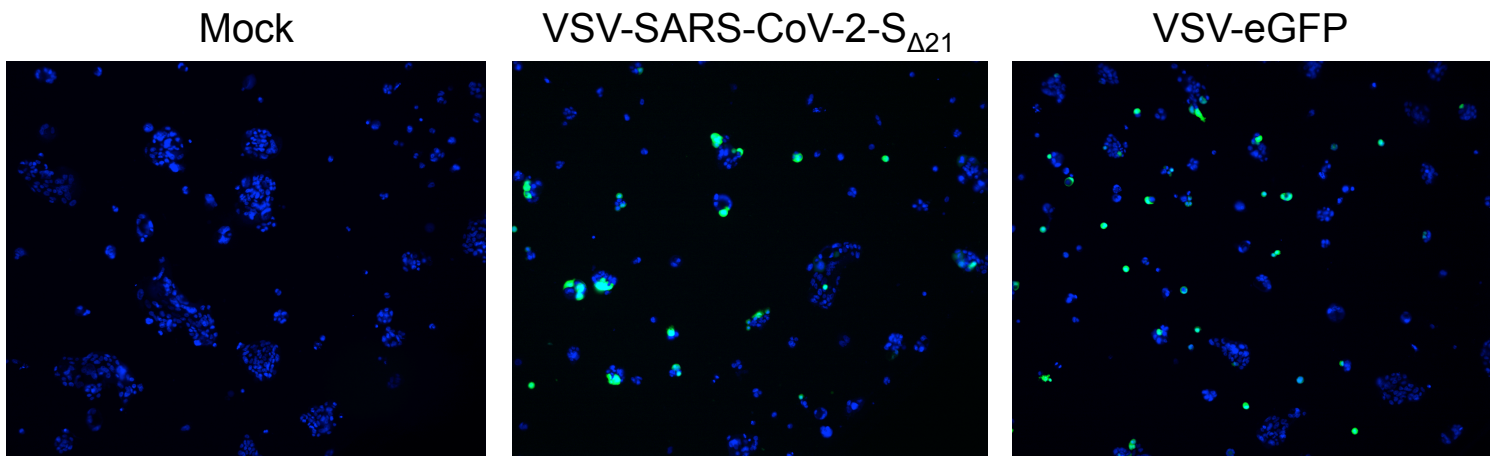
Figure S2. VSV-SARS-CoV-2-S$_{\Delta21}$ can infect human lung adenocarcinoma cells, Related to Figure 1. Calu-3 cells were inoculated with VSV-SARS-CoV-2-S$_{\Delta21}$ or VSV-eGFP at an MA104-calculated MOI of 20. At 7 hpi, cells were stained with the nuclear Hoechst 33342 stain (blue) and images in FITC and DAPI fields (overlaid) were taken using an automated microscope. Representative images from 5 independent experiments are shown.
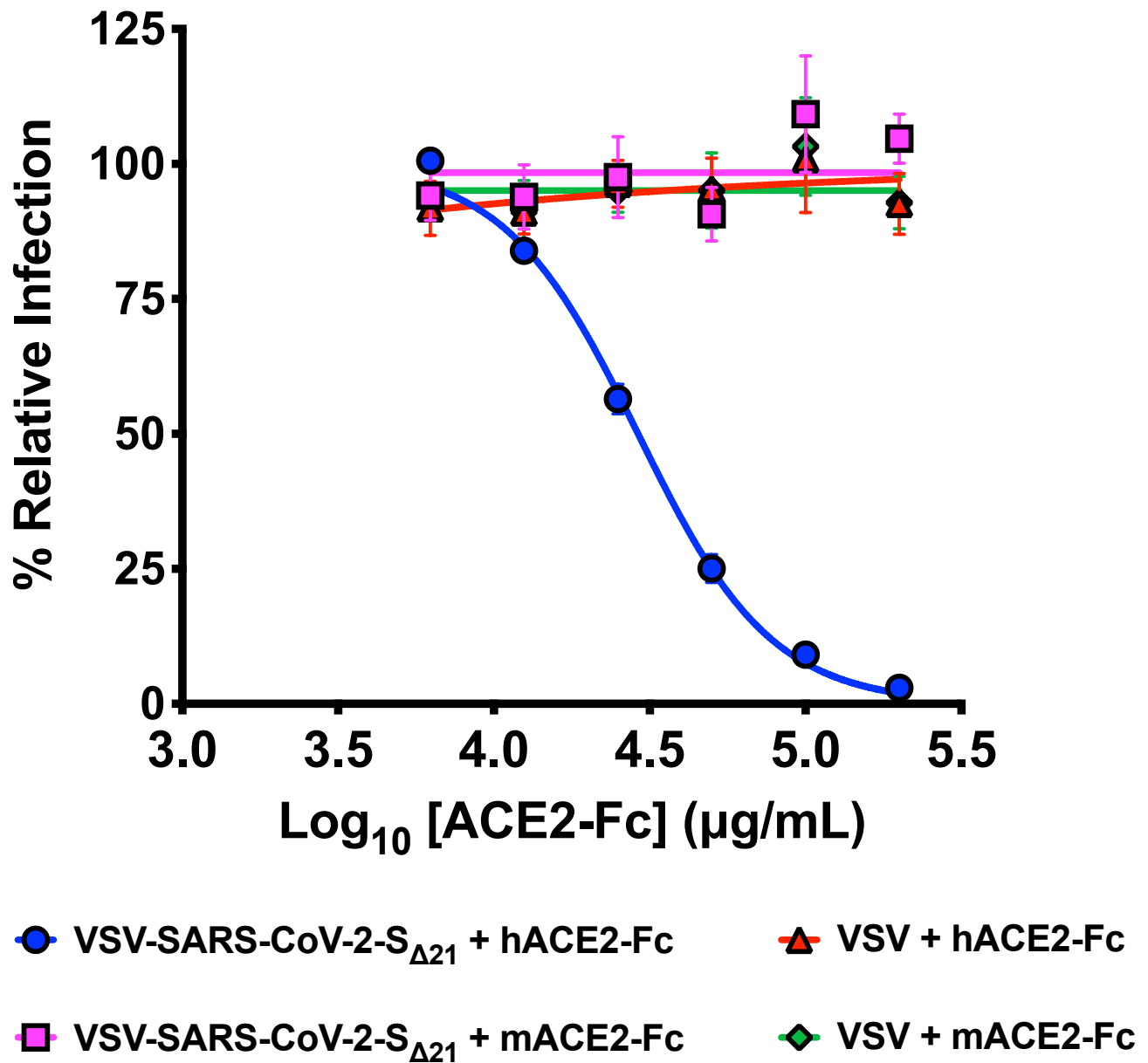
Figure S3. **Inhibition of VSV-SARS-CoV-2-S$_{\Delta21}$ but not VSV with hACE2-Fc receptor decoy proteins, Related to Figure 3.** VSV-SARS-CoV-2-S$_{\Delta21}$ and VSV were incubated with the indicated human or murine ACE2-Fc receptor decoy proteins, and virus-antibody mixtures were used to infect Vero E6 cells in a GRNT assay. Error bars represent the standard error of the mean. Data are representative of three independent experiments.
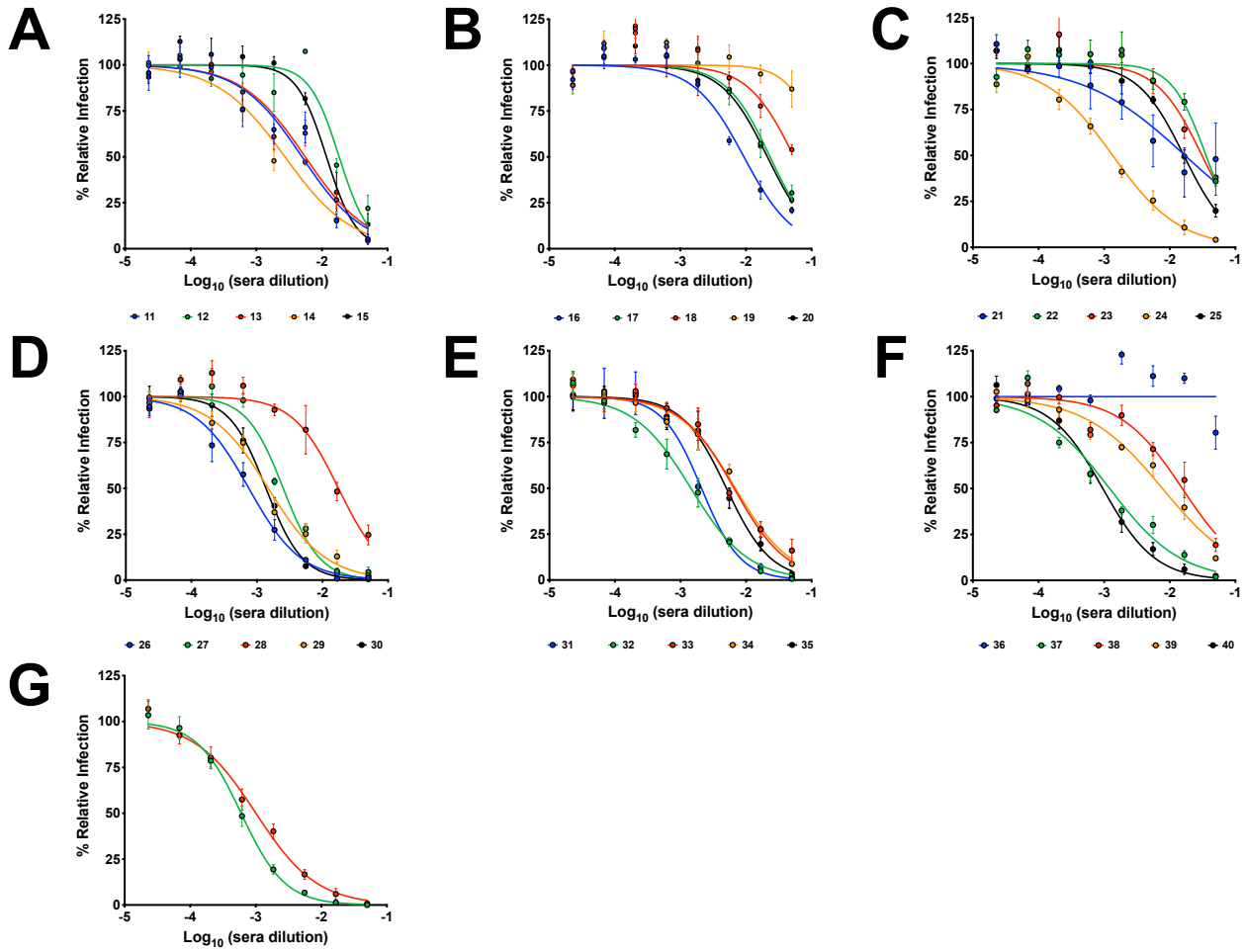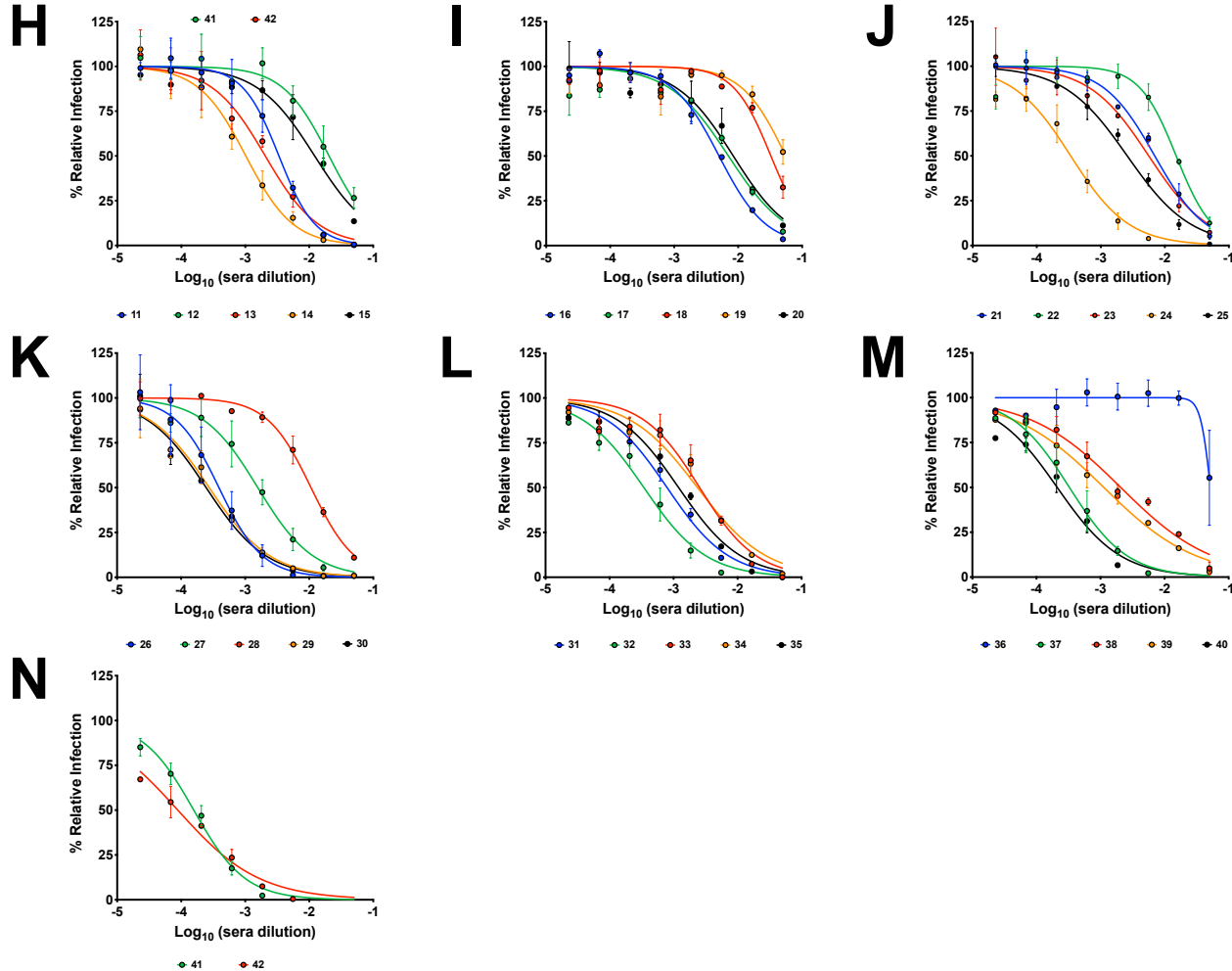
Figure S4. Human immune serum neutralization of SARS-CoV-2 and VSV-SARS-CoV-2-S$_{\Delta21}$, Related to Figure 4. As described in **Fig 4**, human serum samples from PCR confirmed SARS-CoV-2-infected patients were tested in FRNT (**A-G**) and GRNT (**H-N**) assays with SARS-CoV-2 and VSV-SARS-CoV-2-S$_{\Delta21}$. Error bars represent the standard error of the mean.